

1 **Continental-scale biomass redistribution by migratory birds in response to**  
2 **seasonal variation in productivity**

3

4 Wee Hao Ng<sup>1,2\*</sup>, Daniel Fink<sup>2</sup>, Frank A. La Sorte<sup>2</sup>, Tom Auer<sup>2</sup>, Wesley M. Hochachka<sup>2</sup>, Alison Johnston<sup>2,3</sup>,  
5 Adriaan M. Dokter<sup>2</sup>

6 <sup>1</sup> Department of Entomology, Cornell University, Ithaca, NY, USA

7 <sup>2</sup> Cornell Lab of Ornithology, Cornell University, Ithaca, NY, USA

8 <sup>3</sup> Centre for Research into Ecological and Environmental Modelling, University of St Andrews, St  
9 Andrews, UK

10 \* Corresponding author

11

12 **Email addresses**

13 Wee Hao Ng: [wn68@cornell.edu](mailto:wn68@cornell.edu)

Daniel Fink: [daniel.fink@cornell.edu](mailto:daniel.fink@cornell.edu)

14 Frank A. La Sorte: [fal42@cornell.edu](mailto:fal42@cornell.edu)

Tom Auer: [mta45@cornell.edu](mailto:mta45@cornell.edu)

15 Wesley M. Hochachka: [wmh6@cornell.edu](mailto:wmh6@cornell.edu)

Alison Johnston: [aj327@cornell.edu](mailto:aj327@cornell.edu)

16 Adriaan M. Dokter: [amd427@cornell.edu](mailto:amd427@cornell.edu)

17

18 **Acknowledgements**

19 The eBird project relies on the time, dedication, and support from countless individuals and  
20 organizations. We thank the many thousands of eBird participants for their contributions and the eBird  
21 team for their support. This work was funded in part by The Leon Levy Foundation, The Wolf Creek  
22 Foundation and the National Science Foundation (ABI sustaining: DBI-1939187; MSA: DEB-2017817;  
23 computing support from CNS-1059284 and CCF-1522054).

24

25 **Conflict of interest disclosure**

26 All authors have no conflict of interest to declare.

27

28 **Biosketch**

29 Our research team works on statistical analysis and ecological applications of citizen science data and  
30 other large ecological datasets. We create analytical approaches for eBird data that are designed to  
31 enable robust ecological inference on species' distribution, status and trends. We combine hypothesis-  
32 driven questions and newly developed methodological approaches that encompass the full annual cycle  
33 of birds at very large spatial extents. We use this macroecological perspective to address questions on  
34 the role of environmental cues and habitat change on avian distributions and seasonal migration, and  
35 the proximate and ultimate drivers of population changes.

# 1 Continental-scale biomass redistribution by migratory birds in response to 2 seasonal variation in productivity

3  
4 **Short running title:** Bird migration and primary productivity  
5

## 6 **Abstract**

7 **Aim:** Animal migration is often explained as the result of resource tracking in seasonally dynamic  
8 environments. Therefore, resource availability should influence the distributions of migratory animals as  
9 well as their seasonal abundance. We examined the relationship between primary productivity and the  
10 spatio-temporal distributions of migratory birds to assess the role of energy availability in avian migration.

11 **Location:** North America.

12 **Time period:** Full annual cycle, 2011–2016.

13 **Major taxa studied:** Nocturnally migrating landbirds.

14 **Methods:** We used observations of nocturnally migrating landbirds from the eBird community-science  
15 program to estimate weekly spatial distributions of total biomass, abundance, and species richness. We  
16 related these patterns to primary productivity and seasonal productivity surplus estimated using a  
17 remotely-sensed measure of vegetation greenness.

18 **Results:** All three avian metrics showed positive spatial associations with primary productivity, and this  
19 was more pronounced with seasonal productivity surplus. Surprisingly, biomass showed weaker  
20 association than did abundance and richness, despite being a better indicator of energetic requirements.  
21 The strength of associations varied across seasons, being the weakest during migration. During spring  
22 migration, avian biomass increased ahead of vegetation green-up in temperate regions, a pattern also  
23 previously described for herbivorous waterfowl. In the southeastern USA, spring green-up was instead  
24 associated with a net decrease in biomass, and winter biomass greatly exceeded that of summer,  
25 highlighting the region as a winter refuge for short-distance migrants.

26 **Main conclusions:** While instantaneous energy availability is important in shaping the distribution of  
27 migratory birds, the stronger association of productivity with abundance and richness than with biomass  
28 suggests the role of additional drivers unrelated to energetic requirements that are nonetheless  
29 correlated with productivity. Given recent reports of widespread North American avifaunal declines,  
30 including many common species that winter in the southeastern USA, understanding how anthropogenic  
31 activities are impacting winter bird populations in the region should be a research priority.

32  
33 **Keywords:** Abundance, biomass, eBird, North America, productivity, seasonal bird migration, species-  
34 energy relationship, species richness, vegetation greenness  
35

## 36 **1. Introduction**

37 Seasonal variation in resource availability is hypothesized to play a central role in driving avian migration  
38 (Dingle, 2014; Somveille *et al.*, 2015). Migratory bird populations are thought to track seasonal bursts in  
39 primary productivity in the spring to support their migratory journey and subsequent breeding activities.

40 Individual tracking studies have revealed phenological synchronization between spring migration and  
41 vegetation green-up (Kölzsch *et al.*, 2015; Thorup *et al.*, 2017; Lameris *et al.*, 2018; Briedis *et al.*, 2020),  
42 with spring arrivals timed to facilitate a nesting schedule where peak resource availability coincides with  
43 the critical chick growth phase (van der Graaf *et al.*, 2006). Population-level studies have also revealed  
44 synchronization between vegetation greenness and bird occurrence during spring and autumn migration  
45 across a range of dietary guilds, with the strongest evidence found among herbivores and granivores (La  
46 Sorte & Graham, 2021). Additionally, vegetation phenology is also thought to play a prominent role in the  
47 looped annual migration paths of some migratory landbird species (La Sorte *et al.*, 2014). Even outside  
48 the main migratory periods, resource availability has been identified as a potential driver of avian  
49 movement between sites during the winter (Koleček *et al.*, 2018; Knight *et al.*, 2019).

50 These species-level associations between occurrence and primary productivity are expected to  
51 lead to emergent patterns at the community level, such as a higher number of species and individuals  
52 occurring during the breeding season in regions with higher plant productivity. Indeed, many community-  
53 level studies have found strong positive relationships between productivity and species richness,  
54 henceforth called the species-energy relationship (Evans *et al.*, 2005). Yet, the presumed relationships  
55 between productivity, and the net avifaunal abundance and biomass remain relatively unexplored,  
56 despite their potential roles in elucidating the species-energy relationship. For example, the “more  
57 individuals hypothesis” (Wright, 1983; Srivastava & Lawton, 1998) postulates that energy availability limits  
58 the total number of individuals that can be supported in a community, which in turn influences species  
59 richness, since larger population sizes reduce the risk of stochastic extinctions. One key prediction of this  
60 hypothesis is that the abundance-energy relationship should be *stronger* than the species-energy  
61 relationship (Currie *et al.*, 2004; Storch, 2012; Storch *et al.*, 2018). Comparing the strength of these two  
62 relationships would therefore allow us to evaluate this prediction. Moreover, if energy were indeed the  
63 limiting resource shaping the distribution of individuals across space, then since individual energetic needs  
64 generally increase with body size (Daan *et al.*, 1990; Nagy *et al.*, 1999), total avian biomass should reflect  
65 energy requirements of a community better than total abundance (especially if body mass has been  
66 transformed to account for allometric relationships), and hence show an even stronger relationship with  
67 productivity.

68 Another consideration is that migratory birds compete not only with other migratory species for  
69 resources, but also with species that are year-round residents. It has been hypothesized that the  
70 distribution of breeding migratory birds are shaped not by absolute resource levels, but rather by the  
71 seasonal resource surplus that is not fully utilized by resident species (Hurlbert & Haskell, 2003). Since  
72 resident populations are themselves limited by the period of lowest resource availability, the seasonal  
73 productivity difference (the productivity level above the site minimum) is likely to be a better estimate of  
74 resource available to migrants than productivity alone. We would then expect an even stronger  
75 association between biomass and this seasonal productivity difference.

76 Another motivation for considering net abundance and biomass is to understand how different  
77 geographical regions are being utilized by migratory birds across the annual cycle at the community level  
78 (Bauer & Hoyer, 2014). Breeding and wintering ranges are typically described for individual species, but  
79 identifying analogous regions at the community level is complicated by interspecific differences in  
80 migration strategies and abundance patterns. By assessing macroecological patterns of abundance and  
81 biomass year-round, we expect areas used solely as breeding grounds to show a positive temporal  
82 correlation between productivity and abundance or biomass, whereas areas used as wintering grounds  
83 may host higher numbers of birds during winter when productivity is locally at a minimum (La Sorte &  
84 Graham, 2021). Hence, a systematic evaluation of the abundance-productivity and biomass-productivity

85 relationships across the annual cycle would highlight the role of different regions in the ecology of avian  
86 communities.

87 Despite the interest in understanding macroecological relationships between biomass and  
88 primary productivity, most empirical studies have focused on the relationship between spatial patterns  
89 of species richness and vegetation greenness or other measures of productivity (Currie, 1991; Blackburn  
90 & Gaston, 1996; Hurlbert & Haskell, 2003; Evans *et al.*, 2006; Rahbek *et al.*, 2007), and only during part of  
91 the annual cycle (usually the breeding season) over limited spatial extents. The scarcity of large-scale  
92 studies on abundance-productivity and biomass-productivity relationships for migratory birds is due in  
93 part to data constraints. For example, species richness is typically estimated using range maps, which tend  
94 to be readily available. Range maps, however, provide coarse estimates of extent of occurrence and lack  
95 information on patterns of abundance or biomass within the range (Hurlbert & White, 2005; Hurlbert &  
96 Jetz, 2007; Jetz *et al.*, 2008; Gaston & Fuller, 2009). Satellite or telemetry tracking datasets provides  
97 information on patterns of occurrence within the range, but these data sources are necessarily  
98 constrained to a few individuals from a limited number of often large-bodied species, making it hard to  
99 examine population- and community-level patterns of abundance and biomass. Similarly, available  
100 abundance datasets have traditionally been relatively sparse with limited spatial and/or temporal  
101 coverage, since surveys of total abundance across many species and large spatial extents across the full  
102 annual cycle require enormous effort. Large-scale volunteer-based datasets such as eBird (Sullivan *et al.*,  
103 2014) can satisfy these data requirement due to their extensive spatio-temporal coverage.

104 In this study, we explore the relationships between primary productivity and the species richness,  
105 abundance, and biomass of nocturnally migrating landbird species across the annual cycle within North  
106 America. We estimated the three avian ecological metrics using observations from the eBird community-  
107 science program (Sullivan *et al.* 2014), and primary productivity using a remotely-sensed measure of  
108 vegetation greenness, the Enhanced Vegetation Index (EVI; Huete *et al.*, 1994). We assessed the  
109 relationships using spatial correlations between distribution patterns calculated weekly across the annual  
110 cycle, and temporal correlations between time series calculated at each location across the study area.  
111 Assuming energy availability as the main limitation structuring the distribution of the nocturnal migrants,  
112 we hypothesize that the spatial correlations with the seasonal EVI difference should become progressively  
113 weaker from biomass to abundance to species richness, while still being stronger than the counterparts  
114 based on EVI alone. Finally, we use the patterns of temporal correlations to identify regions used for  
115 wintering and breeding at the community level.

116

## 117 **2. Methods**

### 118 **a. Estimating the total biomass, abundance, and species richness of nocturnally migrating** 119 **landbirds**

#### 120 **i. Avian count data**

121 We acquired avian count data from the 2016 eBird Reference Dataset (Fink *et al.*, 2017) for 176  
122 nocturnally migrating landbird species (Dokter *et al.*, 2018; Rosenberg *et al.*, 2019). We chose to focus on  
123 this group of species because of their generally homogenous detection rates. Reports of diurnal migrants  
124 during migration will include many records of over-flying flocks whose locations do not reflect resource  
125 use at the checklist location, whereas nocturnal migrants reported during the day are usually on the  
126 ground utilizing local resources. Also, diurnal migrants often migrate in large flocks during the day  
127 (Beauchamp, 2011), and hence tend to have higher detectability per individual than nocturnal migrants  
128 that would make comparisons counts of detected nocturnal and diurnal migrants inappropriate.

129 We restricted eBird data to “complete checklists”, where the observers reported counts of all bird  
130 species seen or heard, so that species with no observations could be interpreted as being undetected  
131 rather than being omitted by observer preference (Johnston *et al.*, 2021). We selected checklists from the  
132 period 2006/11/22–2016/12/31 (see Supp. Section S1b for an explanation of the choice of start date),  
133 within the region bounded by 20°–72° N latitude, and 52°–170° W longitude. We outline additional  
134 restrictions in Supp. Section S1a. In the end, a total of 8.1 million checklists were available for analysis,  
135 almost all of which (98%) were diurnal observations. These checklists were used to estimate avian biomass  
136 and abundance across the study area and period, using methods described in the next three subsections.

137

## 138 **ii. Predictor and response variables for biomass and abundance interpolation models**

139 Since eBird checklists are unevenly distributed across space and time, we developed models to interpolate  
140 avian biomass and abundance estimated from the checklists to any location and date within the study  
141 area and period. Species distributions are often structured by the environment, so models that include  
142 environmental predictors typically perform better than purely spatiotemporal interpolation (Elith &  
143 Leathwick, 2009). Additionally, including predictors that describe variation in the observation process can  
144 be used to control for checklist-level variation in detectability, thereby improving model performance  
145 (Hochachka *et al.*, 2012; Johnston *et al.*, 2021).

146 We considered four classes of predictors similar to those described by Fink *et al.* (2020a). The  
147 first class is of five effort predictors describing variation in the observation process: number of observers,  
148 observation duration, distance travelled during observation, observation protocol, and checklist  
149 calibration index (CCI; Kelling *et al.*, 2015; Johnston *et al.*, 2018). Observation protocol indicated whether  
150 the checklist corresponded to a stationary or travelling count (other protocols were removed), while CCI  
151 was a derived index designed to account for heterogeneity in the observation process among observers  
152 and checklists. The second class of predictors were three temporal predictors: start time of the checklist,  
153 day of year, and year of observation. The third class of predictors were topographical predictors estimated  
154 at each checklist location: elevation, eastness and northness, all at a 1 × 1 km spatial resolution. Eastness  
155 and northness combine both slope and aspect to describe the orientation of the surface in three  
156 dimensions (Amatulli *et al.*, 2018). Lastly, the fourth class contained 76 descriptors of landcover and  
157 watercover, again estimated at each checklist location. These 76 predictors consisted of four landscape  
158 metrics used to describe the composition and configuration of each of the 19 cover classes within a 2.8 ×  
159 2.8 km neighborhood around the location. The four landscape metrics were the proportion of each cover  
160 class, the largest continuous patch, patch density, and edge density within each neighborhood, and were  
161 calculated using FRAGSTATS (McGarigal *et al.*, 2012; VanDerWal *et al.*, 2014), based on data (Friedl *et al.*,  
162 2010) from Moderate Resolution Imaging Spectroradiometer data (MODIS; Justice *et al.*, 1998). Landcover  
163 classes were from the University of Maryland (UMD) classifications (Hansen *et al.*, 2000). Water cover  
164 classes were derived from the MODIS data. We also included longitude and latitude as predictors to  
165 account for unexplained spatial variation, bringing the total number of predictors to 89.

166 As response variables for the interpolation models, for each checklist, we estimated the total  
167 biomass detected by the observer(s) by summing the body mass across all individuals reported on the  
168 checklist, using sex-averaged body mass estimate for each species from Dunning (2007). Likewise, we  
169 estimated total detected abundance using the total number of individual birds reported. We also  
170 estimated a third response variable, which we call the total *transformed* biomass, where each body mass  
171 is raised to the power of 2/3 before summing, to account for the allometric relationship between  
172 metabolic rates and body size. We choose a scaling exponent of 2/3 for two reasons. First, empirical  
173 studies on birds often found values closer to 2/3 (Daan *et al.*, 1990; Nagy *et al.*, 1999) than the 3/4 in

174 Kleiber's law (Kleiber, 1961). Second, by analyzing both transformed and untransformed biomass, we  
175 would have explored both limits (2/3 and 1) of the likely range of values from theoretical considerations  
176 (Glazier, 2005; Kooijman, 2010). Finally, we log-transformed these estimates of (transformed) biomass  
177 and abundance to improve their distributional properties for the models.

178

### 179 **iii. Fitting the avian abundance and biomass interpolation models**

180 We modelled the relationship between the predictors and the biomass (or abundance) response using  
181 Spatio-temporal Exploratory Models (STEM; Fink *et al.*, 2010, 2020a). In this modeling framework, the  
182 geographic region and study period are divided into overlapping spatio-temporal blocks called stixels. A  
183 base model is separately fitted to the data within each stixel. The model estimate at any spatio-temporal  
184 point of interest is obtained by averaging across the predictions of all base models within whose stixels  
185 the point had fallen; we call the number of models used in the prediction the ensemble size. The  
186 advantage of using STEM over single model approaches is discussed in Fink *et al.* (2010, 2020a).  
187 Henceforth, we refer to the ensemble of base models as the biomass (or abundance) interpolation model.

188 For our implementation, we used stixels with minimal spatial dimensions  $750 \times 750$  km and fixed  
189 temporal dimension of 21 days based on day number only (i.e. data from all years were present, and inter-  
190 annual differences were accounted for during model fitting; see Supp. Section S1b). We used a random  
191 forest base model (Breiman, 2001), implemented using the *ranger* package (Wright & Ziegler, 2017) in R  
192 (R Core Team, 2018). We further limited the study area to regions with sufficient data to meet the model  
193 requirements (Supp. Section S1c). Additional model details can be found in Supp. Sections S1d–g,  
194 including the use of adaptive spatial sizing of stixels to increase the study area into regions of low data  
195 density (Fink *et al.*, 2013), spatio-temporal subsampling to address the issue of uneven checklist  
196 distributions (Robinson *et al.*, 2018; Fink *et al.*, 2020a; Johnston *et al.*, 2021), and data balancing to  
197 account for the interannual increase in eBird checklist volume (Fink *et al.*, 2020a).

198 We evaluated how model performance varied across the annual cycle using a holdout test set, by  
199 calculating the percentage variance explained for all test data within a 7-day moving window (in steps of  
200 3 days). This test set was split from the training set used for model-fitting at the outset, in a train:test ratio  
201 of 80:20, using a procedure that minimized any potential autocorrelations between the two sets (Supp.  
202 Section S1h). We also adopted a spatial subsampling procedure of the test data to avoid having checklists  
203 from highly-sampled locations dominate the calculations (Supp. Section S1i). The percentage of variance  
204 explained within each window varied between 35–53% (mean = 44%) for the biomass model, and 39–67%  
205 (mean 53%) for the abundance model, with relatively small differences among years (interannual std. dev.  
206 within each window between 1–4% var. explained; Supp. Figure S1).

207

### 208 **iv. Generating weekly avian biomass and abundance maps**

209 We used the fitted biomass interpolation model to generate weekly distribution maps of total detected  
210 biomass, separately for each year from 2011 to 2016. To do so, the fitted model was used to predict the  
211 detected biomass at each location across a  $8.4 \times 8.4$  km mapping grid covering the study region, day  
212 (spaced 7 days apart) and year, based on topographical and land cover values at the grid location, and  
213 assuming a standard sampling effort: a single observer with a high CCI of 4, performing a travelling count  
214 starting at 07:00 local time, for a duration of 1 hr and distance of 1 km. The mapping grid is the same as  
215 the ones used in eBird Status and Trends data products (eBird S&T; Fink *et al.*, 2020b). The values of the  
216 effort variables were chosen to reduce the underestimation caused by nondetection and hence bring the  
217 predicted values closer to the unknown true values: for instance, observers with high CCI tended to detect

218 species at a higher rate (Johnston *et al.*, 2018). While even longer durations or distances might also  
219 increase detection, they tended to be less common among checklists, so predictions at these values may  
220 be less accurate. Similar weekly maps were generated for total detected abundance. Since the estimates  
221 were based on standardized sampling efforts, they are expected to correlate well with the true biomass  
222 and abundance values despite variation in effort.

223

#### 224 **v. Generating weekly species richness maps**

225 We generated weekly maps of species richness by using species-level estimates of (non)occurrence from  
226 the 2018 eBird S&T to determine the number of nocturnally migrating species present at each mapping  
227 grid location. In the eBird S&T estimates, the sampling protocols have been optimized separately for each  
228 species to maximize detection, so we expect these estimates to reflect the true occurrence patterns better  
229 than if a single sampling protocol had been applied across all species. This approach also avoids issues  
230 involving equalization (Roswell *et al.*, 2021) that a STEM model for species richness (analogous to the ones  
231 for biomass and abundance) would have to address. On the other hand, this also meant that eBird S&T  
232 abundance estimates are not comparable between species, which was why we did not use them earlier  
233 on for total biomass or abundance. In addition, we wanted multiple years of biomass and abundance  
234 estimates to account for year-to-year variations in the subsequent analyses, whereas eBird S&T estimates  
235 were only available for selected years and also not designed for multi-year analyses. (Year-to-year  
236 variations in richness outside the migratory period were less likely since that would require local  
237 extinctions, so the inability to perform multi-year analyses was less of a concern.)

238

#### 239 **b. Primary productivity**

240 We estimated primary productivity using the Enhanced Vegetation Index (EVI; Huete *et al.*, 1994) derived  
241 from MODIS data. EVI measures canopy greenness, a composite property of canopy structure, leaf area  
242 and canopy chlorophyll content while minimizing soil and atmosphere influences (Myneni *et al.*, 1995).  
243 EVI is less prone to saturation than the Normalized Difference Vegetation Index (NDVI) in high biomass  
244 regions (e.g. Huete *et al.*, 2006), and EVI has been found to correlate well with gross primary production  
245 directly measured from eddy covariance towers (Rahman *et al.*, 2005). We used EVI estimates generated  
246 by La Sorte & Graham (2021) using 16-day 1-km Level-3 MODIS products MOD13A2 V.006 and  
247 MYD13A294 V.006, which combined gave estimates every 8 days. The data were aggregated to a spatial  
248 resolution of 10 × 10 km, and then interpolated to obtain daily estimates using generalized additive  
249 models based on cyclic penalized cubic regression splines (Wood, 2017). From the resulting surface of  
250 estimates, weekly EVI values at each mapping grid location were obtained by bilinear interpolation, using  
251 the *raster* package in R (Hijmans, 2021).

252

#### 253 **c. Associations between primary productivity and biomass, abundance, and species richness.**

254 We examined the association of primary productivity with (transformed) biomass, abundance, and  
255 species richness using two approaches. First, for each week's estimates we calculated the correlation  
256 coefficient between EVI and each of the three ecological metrics by treating the values at each grid  
257 location as paired data points (hereafter "spatial correlation coefficients"). Changing correlations among  
258 weeks would reveal seasonal changes in the spatial associations. Second, at each mapping grid location,  
259 we calculated the temporal cross-correlation coefficient between EVI and each separate ecological metric,  
260 using the time series of the two variables from that location. We did this to reveal any regional differences  
261 in the local temporal associations. We used the Kendall rank correlation coefficient in both analyses

262 (Kendall, 1938), based on the fast algorithm implemented in the *pcaPP* package in R (Filzmoser *et al.*,  
263 2018). These correlation coefficients were intended as descriptive indices describing the degree of  
264 similarity between two *fitted distributions*, and not as statistics for inference; therefore, their values  
265 should not be compared against those from studies designed for inference (e.g. Currie *et al.*, 2004). We  
266 chose Kendall correlation over other measures of distributional (dis)similarity such as earth mover's  
267 distance, because we wanted a rank-based measure to allow for monotonic but nonlinear relationship  
268 between EVI and the ecological metrics. We found no qualitative differences when we used Spearman  
269 correlation coefficients instead.

270 As seasonal resource surplus may play a more important role in shaping the distribution of  
271 breeding migratory birds than the absolute resource level, we repeated the above analysis of spatial  
272 correlations, but this time using seasonal EVI difference in place of EVI. The seasonal EVI difference is  
273 defined as the difference between EVI and its site seasonal minimum (see Supp. Section S2). During the  
274 winter period, most locations had EVI values close to the site minima (Supp. Figure S2), leading to low EVI  
275 difference throughout most of the study area. As a result, spatial correlations with seasonal EVI difference  
276 during this period could be misleading (see Supp. Section S2), so we only calculated the correlations for  
277 each week in a half-year period spanning May to September. We did not repeat the analysis of temporal  
278 associations, since the offset by the site minima would have no effect on the results.

279 To better understand regional differences in the local temporal associations between EVI and  
280 ecological metric (second approach), we looked at the summary times series of each variable from two  
281 regions: the Northeast, which showed highly positive temporal correlation, and the Southeast, which  
282 showed highly negative correlation. Each region was defined using a combination of Bird Conservation  
283 Regions (BCR; Sauer *et al.*, 2003), with the Northeast comprising BCRs 12 and 14, and the Southeast  
284 comprising BCRs 25–27, 31 and 37. For each region and week, we summarized each variable using the  
285 median and inter-quantile range across all locations within that region.

286 Finally, the analysis of temporal associations highlighted regions in the study area where the  
287 correlation coefficients were positive, and regions where they were negative. To determine whether these  
288 regional patterns were associated with climatic factors, we fitted a random forest model with the  
289 temporal correlation coefficients at each mapping grid location as the response, and 19 bioclimatic  
290 variables (WorldClim version 2.1; Fick & Hijmans, 2017) as predictors. Permutation importance was then  
291 evaluated for each bioclimatic variable. However, since many of these bioclimatic predictors were highly  
292 correlated, permutation-based importance metrics may be misleading (Hooker & Mentch, 2019), so we  
293 also used a forward stepwise selection approach where during each step, the variable that resulted in the  
294 largest decrease in out-of-bag mean squared error was added to the existing list of variables. The  
295 sequence in which the variables were added hence indicated their importance, in terms of how much  
296 additional predictive information each variable provided beyond that of variables earlier in the sequence;  
297 the goal was to facilitate a parsimonious bioclimatic description of the temporal association patterns.

298

### 299 **3. Results**

#### 300 **a. Weekly distributions of total avian biomass, abundance, and species richness, and their** 301 **spatial correlations with primary productivity**

302 The weekly distribution maps for biomass, abundance and species richness captured seasonal  
303 migration, with a northward shift of nocturnally migrating landbirds species during spring migration and  
304 a southward shift during autumn migration (Figures 1a, b and c). EVI distributions followed a similar  
305 pattern of northwards vegetation green-up in the spring and southwards vegetation senescence in



306 autumn (Figure 1d). Nonetheless, there were noticeable differences in the spatial patterns among these  
307 quantities, especially outside winter. During summer, both avian (transformed) biomass and abundance  
308 were mostly concentrated along a mid-latitude band between 35° – 45° N latitude of central and eastern  
309 North America (July 6 in Figure 1a, b and Supp. Figure 3a), whereas species richness was mostly  
310 concentrated in the Northeast (Figure 1c). In contrast, EVI displayed a mostly longitudinal pattern, without  
311 any pronounced latitudinal concentration in the east (Figure 1d). However, after subtracting by the  
312 minimum site EVI, the seasonal EVI difference showed closer agreement with the biomass and abundance  
313 latitudinal patterns (Supp. Figure S3b). During spring migration, biomass, abundance and richness were  
314 all distributed more northerly than both EVI and the seasonal EVI difference (May 25 in Figure 1 and Supp.  
315 Figure S3).

316 Weekly evaluations of the spatial correlation coefficient between (transformed) biomass and EVI  
317 across the study area revealed seasonal variation in the strength of spatial association across the annual  
318 cycle (Figure 1e and Supp. Figure S3c). The correlation was strongest between March and April (early  
319 spring migration), and weakest between September and October (the middle of autumn migration).  
320 Between mid-March and late May, biomass increased well ahead of EVI in the Northern Great Plains,  
321 whereas in the Southeast, biomass decreased even when EVI remained relatively high (Figures 1a, d).  
322 These changes increased the mismatch between biomass and EVI, hence causing the decrease in  
323 correlation seen over that period (Supp. Figure S4). The subsequent increase in correlation until early July  
324 could be attributed to EVI “catching up” with the biomass levels in the north and hence reducing the  
325 mismatch.

326 Similar patterns of seasonal variations were also observed in the associations between EVI and  
327 total abundance and species richness, although with quantitative differences in the strength of  
328 associations (Figure 1e and Supp. Figure S3c). EVI was more strongly correlated with richness than biomass  
329 or abundance throughout most of the annual cycle. Correlation with abundance was stronger than  
330 biomass during summer, whereas the reverse was true during fall migration.

331 The spatial correlations showed qualitatively similar dynamics when EVI was replaced by the  
332 seasonal EVI difference, with a peak mid-summer and sharp decreases in correlation during the migratory  
333 periods (Figure 1f and Supp. Figure S3d). The correlations were also generally higher than the EVI  
334 counterparts during the breeding season. Among the three metrics, seasonal EVI difference showed  
335 marginally higher correlation with abundance than with richness or (transformed) biomass.

336

## 337 **b. Temporal association between avian biomass and primary productivity**

338 Figure 2a shows the full-year temporal association between EVI and biomass, with the color at each  
339 location representing the value of the Kendall coefficient calculated at the location. The sign of the  
340 association was generally determined by the climatic zone, with positive association in the temperate  
341 zone to the north, and negative association in the subtropical zone to the south. We observed the same  
342 qualitative patterns using Pearson and Spearman correlation coefficients (Supp. Figures S6a, b). Patterns  
343 of temporal association were also similar for abundance (Supp. Fig S7).

344 In the Northeast, both biomass and EVI were highest in spring and summer, and lowest in winter  
345 (Figure 2b), hence the positive association in this region. Note however, that the changes in biomass and  
346 EVI were not synchronous. In particular, we found that biomass increased most rapidly in April and peaked  
347 in mid-May, nearly a month ahead of EVI. Similarly, observed biomass decreased earlier in autumn than  
348 EVI. In the Southeast, the pattern was reversed, and spring green-up was associated with a drop in  
349 biomass (Figure 2c). Biomass started to decrease in March, reaching its lowest levels in summer and early

350 autumn, before increasing again around October and peaking in winter. The opposite temporal trends  
351 between EVI and biomass hence explained the negative temporal association in the Southeast.

352 Forward stepwise selection (Supp. Figure S8a) revealed that the two bioclimatic variables that  
353 best predicted the spatial patterns of temporal associations between EVI and biomass were BIO11 (mean  
354 temperature of coldest quarter), followed by BIO18 (precipitation of warmest quarter), explaining 92% of  
355 the variations in the Kendall coefficients. There were strong positive seasonal associations between  
356 biomass and productivity where winters are cold (BIO11 was low), and strong negative associations in  
357 regions with mild winters and wet summers (both BIO11 and BIO18 were high), see Figure 3. Additional  
358 results from both forward stepwise selection and permutation importance can be found in Supp. Section  
359 S3 and Supp. Figures S8–S10.

360

#### 361 **4. Discussion**

362 Our analyses have revealed broad-scale positive associations of primary productivity with the biomass,  
363 abundance, and species richness of nocturnally migrating landbirds across space and time. Under a  
364 scenario of resource tracking by migrants, in which energy availability is the main factor and proximate  
365 cue determining the spatial distribution of migratory landbirds, one would expect primary productivity to  
366 be more closely associated with biomass than abundance, because abundance does not reflect the higher  
367 energetic needs of larger birds (Daan *et al.*, 1990; Nagy *et al.*, 1999). The relationship between productivity  
368 and richness (Currie *et al.*, 2004; Storch, 2012; Storch *et al.*, 2018) is expected to be even more indirect  
369 and therefore weaker, as it depends on complex and diverse mechanisms that can weaken the  
370 relationship. For example, the “more-individuals hypothesis” (Wright, 1983; Srivastava & Lawton, 1998)  
371 suggests that high energy availability allows more individuals to be supported, which in turn reduces the  
372 risk of stochastic extinction and hence leads to higher species richness. A key prediction from this  
373 hypothesis is that the relationship with productivity should be stronger for abundance than diversity, since  
374 the second relationship is more distal.

375 Contrary to these expectations, instead of associations with productivity becoming progressively  
376 weaker from biomass to abundance to species richness, we found the opposite pattern (Figure 1e), with  
377 species richness more strongly correlated with productivity compared to (transformed) biomass or  
378 abundance. These findings are replicated in studies of other taxa where richness is often more strongly  
379 correlated with productivity compared to abundance (Currie *et al.*, 2004; Storch *et al.*, 2018). In contrast,  
380 the seasonal surplus in productivity did show a marginally stronger correlation with abundance than  
381 richness, although the correlation with biomass remained lowest. Since each metric showed higher  
382 correlation with the productivity surplus than with absolute productivity during the breeding season,  
383 productivity surplus is likely a better measure of energy available to migratory birds than productivity  
384 alone, by better accounting for competition and resource use by resident species and other non-avian  
385 taxa (Hurlbert & Haskell, 2003; Somveille *et al.*, 2018). Nonetheless, the fact that biomass still showed a  
386 lower correlation than abundance (despite being a more accurate indicator of energetic requirements)  
387 merits explanation. Besides energy availability, the spatial distribution of breeding birds may also be  
388 influenced by other limitations such as the availability and structural diversity of nesting habitats, which  
389 are often correlated with productivity (Dobson *et al.*, 2015) and can hence enhance the productivity-  
390 abundance association. Moreover, abundance and biomass patterns are likely to be driven more by  
391 common species, which may have idiosyncratic requirements unrelated to energy availability, such as nest  
392 sites. Finally, many nocturnally migrating bird species do not directly consume primary production; while  
393 higher primary productivity likely leads to higher resource availability across trophic levels, the association  
394 need not always be perfect (Piersma, 2020). Hence, one possible refinement of our analysis would be to

395 decompose avian biomass by dietary guilds and to study the spatial associations with productivity at the  
396 guild level (La Sorte & Graham, 2021).

397 We also found strong seasonal variation in the spatial association between productivity and the  
398 three ecological metrics (Figure 1e). Across the annual cycle, biomass was most strongly correlated with  
399 EVI during late winter: even though EVI was generally low across the continent, it remains relatively high  
400 in the Southeast, which is also the region where migrants were concentrated in winter, suggesting  
401 immediate and strong constraints by resource availability during this time of the year. The correlation  
402 decreased during spring migration as migrants overtook the wave of spring green-up, and then increased  
403 during subsequent green-up in summer, a pattern visible in both in the correlations with EVI and surplus  
404 EVI. This phenological lag in vegetation greenness relative to biomass can also be seen in Figure 2b, with  
405 biomass building up ahead of EVI in the Northeast during spring. Such a pattern of overtaking the “green  
406 wave” has been documented with migratory geese (Kölzsch *et al.*, 2015). Early arrival on breeding grounds  
407 prior to green-up is usually explained by selection for timing of breeding that aligns the resource  
408 requirements of nestlings with peak resource availability (Kölzsch *et al.*, 2015; Fokkema *et al.*, 2020). Our  
409 findings suggest that this explanation also generalizes to nocturnally migratory landbirds (Both *et al.*,  
410 2010). Both the higher overall *absolute* productivity level and the ability of migratory birds to accumulate  
411 and carry large body reserves to fuel migration and initial breeding activities (Sandberg, 2008) would allow  
412 the migrants to (temporarily) deviate from the instantaneous *relative* energy landscape. The relationships  
413 between productivity and the three ecological metrics fell again during fall migration: much of the biomass  
414 stayed along the mid-latitude band while EVI was falling in the north due to leaf senescence, hence shifting  
415 the EVI distribution southward. This lower association also suggests that the migrants may be less  
416 constrained by instantaneous energy availability during this phase of the annual cycle (Briedis *et al.*, 2020;  
417 Horton *et al.*, 2020).

418 Seasonal shifts in the biomass distributions (Figure 1a) also led to unexpected patterns in the local  
419 temporal associations with EVI across the annual cycle (Figure 2a). Large populations of nocturnally  
420 migrating landbirds were found to aggregate in the subtropical regions of Southeast during winter.  
421 However, in these regions, spring greening was instead accompanied by a net decrease in total biomass  
422 (Figure 2c), due to the northward mass exodus of overwintering populations that the influx of Neotropical  
423 migrants could not compensate for. Increased productivity of the environment is therefore associated  
424 with a decrease rather than an increase in migrant biomass; hence the negative temporal association in  
425 these regions. The southeastern subtropical region thus plays the role of a winter refuge for many species  
426 of nocturnally migrating landbirds in North America, as also seen from the fewfold increase in abundance  
427 and biomass during winter (Figures 2c, S7c). Our analysis of bioclimatic variables showed that regions with  
428 negative local temporal associations were primarily characterized by mild winters and wet summers  
429 (Figure 3b). While this could be related to a higher winter productivity and hence food availability  
430 compared to the more northerly regions (Figure 1d), the mild winter conditions likely also play a role by  
431 reducing thermoregulatory costs (Cartar & Morrison, 1997).

432 We acknowledge a number of limitations with our approach. First, since the biomass and  
433 abundance interpolation models were fitted using observation data, the model estimates could have been  
434 affected by the detectability of the birds. In particular, the lower biomass estimates in Figures 2b and c  
435 during August and early September (compared to June and July) were likely affected by a decrease in  
436 detectability commonly observed during breeding and moult. Nonetheless, this should not affect the  
437 spatial correlations, which only depended on the relative values between different locations in the same  
438 week. Second, richness was obtained using a different approach (eBird S&T estimates) from the biomass  
439 and abundance estimates (STEM), which may affect the comparison between the strength of their spatial  
440 associations with productivity. Third, STEM included land cover predictors which may themselves affect

441 EVI, so there is a risk of circularity when analyzing correlations with EVI. However, this risk was minimized  
442 by the use of flexible base models together with many predictors that affect EVI in different ways, so the  
443 models were not constrained to learn EVI-related signals. Fourth, due to the tradeoff between coverage  
444 and accuracy, our study area did not include Central America nor the high latitudes where some of the  
445 nocturnal migratory species spend their wintering/breeding seasons. Finally, it is worth repeating that the  
446 correlation coefficients were meant as measures of similarity between two fitted distributions, so they  
447 should not be compared to values from studies designed for statistical inference.

448 Our findings highlight the role of the Southeast as winter refuge for short-distance migrants,  
449 which make up a large proportion of migratory landbird biomass in North America. Parts of coastal  
450 California and the Central Valley likely play a similar role for the western US. While many of the species  
451 wintering within the contiguous US are regarded as common, recent work on North American avifauna  
452 population trends (Rosenberg *et al.*, 2019) have shown that they are nonetheless experiencing steep  
453 declines. Many studies have focused on the importance of protecting wintering habitats for the  
454 conservation of Neotropical migratory species (e.g. Sherry & Holmes, 1996; Faaborg *et al.*, 2010), but  
455 relatively little is known about the impact of wintering refuge availability and quality on the long-term  
456 population trends of the short-distance migrants. We hope that our results can spur more work in this  
457 direction.

458

## 459 References

- 460 Amatulli, G., Domisch, S., Tuanmu, M.-N., Parmentier, B., Ranipeta, A., Malczyk, J. & Jetz, W.  
461 (2018) A suite of global, cross-scale topographic variables for environmental and  
462 biodiversity modeling. *Scientific Data*, **5**, 180040.
- 463 Bauer, S. & Hoyer, B.J. (2014) Migratory Animals Couple Biodiversity and Ecosystem  
464 Functioning Worldwide. *Science*, **344**, 1242552.
- 465 Beauchamp, G. (2011) Why migrate during the day: a comparative analysis of North American  
466 birds. *Journal of Evolutionary Biology*, **24**, 1969–1974.
- 467 Blackburn, T.M. & Gaston, K.J. (1996) Spatial patterns in the species richness of birds in the  
468 New World. *Ecography*, **19**, 369–376.
- 469 Both, C., Van Turnhout, C.A.M., Bijlsma, R.G., Siepel, H., Van Strien, A.J. & Foppen, R.P.B.  
470 (2010) Avian population consequences of climate change are most severe for long-  
471 distance migrants in seasonal habitats. *Proceedings of the Royal Society B: Biological*  
472 *Sciences*, **277**, 1259–1266.
- 473 Breiman, L. (2001) Random Forests. *Machine Learning*, **45**, 5–32.
- 474 Briedis, M., Bauer, S., Adamík, P., Alves, J.A., Costa, J.S., Emmenegger, T., Gustafsson, L.,  
475 Koleček, J., Krist, M., Liechti, F., Lisovski, S., Meier, C.M., Procházka, P. & Hahn, S.  
476 (2020) Broad-scale patterns of the Afro-Palaeartic landbird migration. *Global Ecology*  
477 *and Biogeography*, **29**, 722–735.
- 478 Cartar, R.V. & Morrison, R.I.G. (1997) Estimating metabolic costs for homeotherms from  
479 weather data and morphology: an example using calidridine sandpipers. *Canadian*  
480 *Journal of Zoology*, **75**, 94–101.
- 481 Currie, D.J. (1991) Energy and Large-Scale Patterns of Animal- and Plant-Species Richness. *The*  
482 *American Naturalist*, **137**, 27–49.
- 483 Currie, D.J., Mittelbach, G.G., Cornell, H.V., Field, R., Guégan, J.-F., Hawkins, B.A., Kaufman,  
484 D.M., Kerr, J.T., Oberdorff, T., O'Brien, E. & Turner, J.R.G. (2004) Predictions and tests

485 of climate-based hypotheses of broad-scale variation in taxonomic richness. *Ecology*  
486 *Letters*, **7**, 1121–1134.

487 Daan, S., Masman, D. & Groenewold, A. (1990) Avian basal metabolic rates: their association  
488 with body composition and energy expenditure in nature. *American Journal of*  
489 *Physiology-Regulatory, Integrative and Comparative Physiology*, **259**, R333–R340.

490 Dingle, H. (2014) *Migration: the biology of life on the move*, Second edition. Oxford University  
491 Press, Oxford ; New York.

492 Dobson, L.L., Sorte, F.A.L., Manne, L.L. & Hawkins, B.A. (2015) The diversity and abundance  
493 of North American bird assemblages fail to track changing productivity. *Ecology*, **96**,  
494 1105–1114.

495 Dokter, A.M., Farnsworth, A., Fink, D., Ruiz-Gutierrez, V., Hochachka, W.M., La Sorte, F.A.,  
496 Robinson, O.J., Rosenberg, K.V. & Kelling, S. (2018) Seasonal abundance and survival  
497 of North America’s migratory avifauna determined by weather radar. *Nature Ecology &*  
498 *Evolution*, **2**, 1603–1609.

499 Dunning, J. (2007) *CRC Handbook of Avian Body Masses, Second Edition*, CRC Press.

500 Elith, J. & Leathwick, J.R. (2009) Species Distribution Models: Ecological Explanation and  
501 Prediction Across Space and Time. *Annual Review of Ecology, Evolution, and*  
502 *Systematics*, **40**, 677–697.

503 Evans, K.L., James, N.A. & Gaston, K.J. (2006) Abundance, species richness and energy  
504 availability in the North American avifauna. *Global Ecology and Biogeography*, **15**, 372–  
505 385.

506 Evans, K.L., Warren, P.H. & Gaston, K.J. (2005) Species-energy relationships at the  
507 macroecological scale: a review of the mechanisms. *Biological Reviews*, **80**, 1–25.

508 Faaborg, J., Holmes, R.T., Anders, A.D., Bildstein, K.L., Dugger, K.M., Gauthreaux, S.A.,  
509 Heglund, P., Hobson, K.A., Jahn, A.E., Johnson, D.H., Latta, S.C., Levey, D.J., Marra,  
510 P.P., Merkord, C.L., Nol, E., Rothstein, S.I., Sherry, T.W., Sillett, T.S., Thompson, F.R.  
511 & Warnock, N. (2010) Conserving migratory land birds in the New World: Do we know  
512 enough? *Ecological Applications*, **20**, 398–418.

513 Fick, S.E. & Hijmans, R.J. (2017) WorldClim 2: new 1-km spatial resolution climate surfaces for  
514 global land areas. *International Journal of Climatology*, **37**, 4302–4315.

515 Filzmoser, P., Fritz, H. & Kalcher, K. (2018) *pcaPP: Robust PCA by Projection Pursuit*.  
516 <https://CRAN.R-project.org/package=pcaPP>

517 Fink, D., Auer, T., Johnston, A., Ruiz-Gutierrez, V., Hochachka, W.M. & Kelling, S. (2020a)  
518 Modeling avian full annual cycle distribution and population trends with citizen science  
519 data. *Ecological Applications*, **30**, e02056.

520 Fink, D., Auer, T., Johnston, A., Strimas-Mackey, M., Robinson, O., Ligocki, S., Hochachka,  
521 W., Wood, C., Davies, I., Iliff, M. & Seitz, L. (2020b) eBird Status and Trends.

522 Fink, D., Auer, T., Obregon, F., Hochachka, W.M., Iliff, M., Sullivan, B., Wood, C., Davies, I. &  
523 Kelling, S. (2017) The eBird Reference Dataset Version 2016 (ERD2016).

524 Fink, D., Damoulas, T. & Dave, J. (2013) Adaptive spatio-temporal exploratory models:  
525 Hemisphere-wide species distributions from massively crowdsourced ebird data.  
526 *Proceedings of the Twenty-Seventh AAAI Conference on Artificial Intelligence*  
527 AAAI’13., pp. 1284–1290. AAAI Press, Bellevue, Washington.

528 Fink, D., Hochachka, W.M., Zuckerberg, B., Winkler, D.W., Shaby, B., Munson, M.A., Hooker,  
529 G., Riedewald, M., Sheldon, D. & Kelling, S. (2010) Spatiotemporal exploratory models  
530 for broad-scale survey data. *Ecological Applications*, **20**, 2131–2147.

531 Fokkema, W., van der Jeugd, H.P., Lameris, T.K., Dokter, A.M., Ebbing, B.S., de Roos, A.M.,  
532 Nolet, B.A., Piersma, T. & Olf, H. (2020) Ontogenetic niche shifts as a driver of  
533 seasonal migration. *Oecologia*, **193**, 285–297.

534 Friedl, M.A., Sulla-Menashe, D., Tan, B., Schneider, A., Ramankutty, N., Sibley, A. & Huang,  
535 X. (2010) MODIS Collection 5 global land cover: Algorithm refinements and  
536 characterization of new datasets. *Remote Sensing of Environment*, **114**, 168–182.

537 Gaston, K.J. & Fuller, R.A. (2009) The sizes of species' geographic ranges. *Journal of Applied*  
538 *Ecology*, **46**, 1–9.

539 Glazier, D.S. (2005) Beyond the '3/4-power law': variation in the intra-and interspecific scaling  
540 of metabolic rate in animals. *Biological Reviews*, **80**, 611–662.

541 van der Graaf, S., Stahl, J., Klimkowska, A., Bakker, J.P. & Drent, R.H. (2006) Surfing on a  
542 green wave - how plant growth drives spring migration in the Barnacle Goose *Branta*  
543 *leucopsis*. *Ardea*, **94**, 567–577.

544 Hansen, M.C., Defries, R.S., Townshend, J.R.G. & Sohlberg, R. (2000) Global land cover  
545 classification at 1 km spatial resolution using a classification tree approach. *International*  
546 *Journal of Remote Sensing*, **21**, 1331–1364.

547 Hijmans, R.J. (2021) *raster: Geographic Data Analysis and Modeling*. R package version 3.4-  
548 13. <https://CRAN.R-project.org/package=raster>

549 Hochachka, W.M., Fink, D., Hutchinson, R.A., Sheldon, D., Wong, W.-K. & Kelling, S. (2012)  
550 Data-intensive science applied to broad-scale citizen science. *Trends in Ecology &*  
551 *Evolution*, **27**, 130–137.

552 Hooker, G. & Mentch, L. (2019) Please Stop Permuting Features: An Explanation and  
553 Alternatives. *arXiv:1905.03151 [cs, stat]*.

554 Horton, K.G., La Sorte, F.A., Sheldon, D., Lin, T.-Y., Winner, K., Bernstein, G., Maji, S.,  
555 Hochachka, W.M. & Farnsworth, A. (2020) Phenology of nocturnal avian migration has  
556 shifted at the continental scale. *Nature Climate Change*, **10**, 63–68.

557 Huete, A., Justice, C. & Liu, H. (1994) Development of vegetation and soil indices for MODIS-  
558 EOS. *Remote Sensing of Environment*, **49**, 224–234.

559 Huete, A.R., Didan, K., Shimabukuro, Y.E., Ratana, P., Saleska, S.R., Huttyra, L.R., Yang, W.,  
560 Nemani, R.R. & Myneni, R. (2006) Amazon rainforests green-up with sunlight in dry  
561 season. *Geophysical Research Letters*, **33**.

562 Hurlbert, A.H. & Haskell, J.P. (2003) The Effect of Energy and Seasonality on Avian Species  
563 Richness and Community Composition. *The American Naturalist*, **161**, 83–97.

564 Hurlbert, A.H. & Jetz, W. (2007) Species richness, hotspots, and the scale dependence of range  
565 maps in ecology and conservation. *Proceedings of the National Academy of Sciences*,  
566 **104**, 13384–13389.

567 Hurlbert, A.H. & White, E.P. (2005) Disparity between range map- and survey-based analyses of  
568 species richness: patterns, processes and implications. *Ecology Letters*, **8**, 319–327.

569 Jetz, W., Sekercioglu, C.H. & Watson, J.E.M. (2008) Ecological Correlates and Conservation  
570 Implications of Overestimating Species Geographic Ranges. *Conservation Biology*, **22**,  
571 110–119.

572 Johnston, A., Fink, D., Hochachka, W.M. & Kelling, S. (2018) Estimates of observer expertise  
573 improve species distributions from citizen science data. *Methods in Ecology and*  
574 *Evolution*, **9**, 88–97.

575 Johnston, A., Hochachka, W.M., Strimas-Mackey, M.E., Gutierrez, V.R., Robinson, O.J., Miller,  
576 E.T., Auer, T., Kelling, S.T. & Fink, D. (2021) Analytical guidelines to increase the value

577 of community science data: An example using eBird data to estimate species  
578 distributions. *Diversity and Distributions*, **27**, 1265–1277.

579 Justice, C.O., Vermote, E., Townshend, J.R.G., Defries, R., Roy, D.P., Hall, D.K., Salomonson,  
580 V.V., Privette, J.L., Riggs, G., Strahler, A., Lucht, W., Myneni, R.B., Knyazikhin, Y.,  
581 Running, S.W., Nemani, R.R., Zhengming Wan, Huete, A.R., Leeuwen, W. van, Wolfe,  
582 R.E., Giglio, L., Muller, J., Lewis, P. & Barnsley, M.J. (1998) The Moderate Resolution  
583 Imaging Spectroradiometer (MODIS): land remote sensing for global change research.  
584 *IEEE Transactions on Geoscience and Remote Sensing*, **36**, 1228–1249.

585 Kelling, S., Johnston, A., Hochachka, W.M., Iliff, M., Fink, D., Gerbracht, J., Lagoze, C., Sorte,  
586 F.A.L., Moore, T., Wiggins, A., Wong, W.-K., Wood, C. & Yu, J. (2015) Can  
587 Observation Skills of Citizen Scientists Be Estimated Using Species Accumulation  
588 Curves? *PLOS ONE*, **10**, e0139600.

589 Kendall, M.G. (1938) A new measure of rank correlation. *Biometrika*, **30**, 81–93.

590 Kleiber, M. (1961) *The Fire of Life: An Introduction to Animal Energetics*, Wiley, New York,  
591 NY, USA.

592 Knight, S.M., Gow, E.A., Bradley, D.W., Clark, R.G., Bélisle, M., Berzins, L.L., Blake, T.,  
593 Bridge, E.S., Burke, L., Dawson, R.D., Dunn, P.O., Garant, D., Holroyd, G.L., Hussell,  
594 D.J.T., Lansdorp, O., Laughlin, A.J., Leonard, M.L., Pelletier, F., Shutler, D., Siefferman,  
595 L., Taylor, C.M., Trefry, H.E., Vleck, C.M., Vleck, D., Whittingham, L.A., Winkler,  
596 D.W. & Norris, D.R. (2019) Nonbreeding season movements of a migratory songbird are  
597 related to declines in resource availability. *The Auk*, **136**.

598 Koleček, J., Hahn, S., Emmenegger, T. & Procházka, P. (2018) Intra-tropical movements as a  
599 beneficial strategy for Palearctic migratory birds. *Royal Society Open Science*, **5**, 171675.

600 Kölzsch, A., Bauer, S., Boer, R. de, Griffin, L., Cabot, D., Exo, K.-M., Jeugd, H.P. van der &  
601 Nolet, B.A. (2015) Forecasting spring from afar? Timing of migration and predictability  
602 of phenology along different migration routes of an avian herbivore. *Journal of Animal*  
603 *Ecology*, **84**, 272–283.

604 Kooijman, S.A.L.M. (2010) *Dynamic Energy and Mass Budgets in Biological Systems (2nd*  
605 *Edition)*, Cambridge University Press, Cambridge, GBR.

606 La Sorte, F.A., Fink, D., Hochachka, W.M., DeLong, J.P. & Kelling, S. (2014) Spring phenology  
607 of ecological productivity contributes to the use of looped migration strategies by birds.  
608 *Proceedings of the Royal Society B: Biological Sciences*, **281**, 20140984.

609 La Sorte, F.A. & Graham, C.H. (2021) Phenological synchronization of seasonal bird migration  
610 with vegetation greenness across dietary guilds. *Journal of Animal Ecology*, **90**, 343–355.

611 Lameris, T.K., van der Jeugd, H.P., Eichhorn, G., Dokter, A.M., Bouten, W., Boom, M.P.,  
612 Litvin, K.E., Ens, B.J. & Nolet, B.A. (2018) Arctic Geese Tune Migration to a Warming  
613 Climate but Still Suffer from a Phenological Mismatch. *Current Biology*, **28**, 2467-  
614 2473.e4.

615 McGarigal, K., Cushman, S.A. & Ene, E. (2012) *FRAGSTATS v4: spatial pattern analysis*  
616 *program for categorical and continuous maps*.  
617 <http://www.umass.edu/landeco/research/fragstats/fragstats.html>

618 Myneni, R.B., Hall, F.G., Sellers, P.J. & Marshak, A.L. (1995) The interpretation of spectral  
619 vegetation indexes. *IEEE Transactions on Geoscience and Remote Sensing*, **33**, 481–486.

620 Nagy, K.A., Girard, I.A. & Brown, T.K. (1999) Energetics of Free-Ranging Mammals, Reptiles,  
621 and Birds. *Annual Review of Nutrition*, **19**, 247–277.

622 Piersma, T. (2020) Ornithology from the Flatlands. *Ardea*, **108**, 111–114.

623 R Core Team (2018) *R: A language and environment for statistical computing*, R Foundation for  
624 Statistical Computing, Vienna, Austria.

625 Rahbek, C., Gotelli, N.J., Colwell, R.K., Entsminger, G.L., Rangel, T.F.L.V.B. & Graves, G.R.  
626 (2007) Predicting continental-scale patterns of bird species richness with spatially explicit  
627 models. *Proceedings of the Royal Society B: Biological Sciences*, **274**, 165–174.

628 Rahman, A.F., Sims, D.A., Cordova, V.D. & El-Masri, B.Z. (2005) Potential of MODIS EVI and  
629 surface temperature for directly estimating per-pixel ecosystem C fluxes. *Geophysical  
630 Research Letters*, **32**.

631 Robinson, O.J., Ruiz-Gutierrez, V. & Fink, D. (2018) Correcting for bias in distribution  
632 modelling for rare species using citizen science data. *Diversity and Distributions*, **24**,  
633 460–472.

634 Rosenberg, K.V., Dokter, A.M., Blancher, P.J., Sauer, J.R., Smith, A.C., Smith, P.A., Stanton,  
635 J.C., Panjabi, A., Helft, L., Parr, M. & Marra, P.P. (2019) Decline of the North American  
636 avifauna. *Science*, **366**, 120–124.

637 Roswell, M., Dushoff, J. & Winfree, R. (2021) A conceptual guide to measuring species  
638 diversity. *Oikos*, **130**, 321–338.

639 Sandberg, R. (2008) Fat reserves of migrating passerines at arrival on the breeding grounds in  
640 Swedish Lapland. *Ibis*, **138**, 514–524.

641 Sauer, J.R., Fallon, J.E. & Johnson, R. (2003) Use of North American Breeding Bird Survey  
642 Data to Estimate Population Change for Bird Conservation Regions. *The Journal of  
643 Wildlife Management*, **67**, 372–389.

644 Sherry, T.W. & Holmes, R.T. (1996) Winter Habitat Quality, Population Limitation, and  
645 Conservation of Neotropical-Nearctic Migrant Birds. *Ecology*, **77**, 36–48.

646 Somveille, M., Rodrigues, A.S.L. & Manica, A. (2018) Energy efficiency drives the global  
647 seasonal distribution of birds. *Nature Ecology & Evolution*, **2**, 962–969.

648 Somveille, M., Rodrigues, A.S.L. & Manica, A. (2015) Why do birds migrate? A  
649 macroecological perspective. *Global Ecology and Biogeography*, **24**, 664–674.

650 Srivastava, D.S. & Lawton, J.H. (1998) Why More Productive Sites Have More Species: An  
651 Experimental Test of Theory Using Tree-Hole Communities. *The American Naturalist*,  
652 **152**, 510–529.

653 Storch, D. (2012) *Biodiversity and its Energetic and Thermal Controls*. *Metabolic Ecology* (ed.  
654 by R.M. Sibly), J.H. Brown), and A. Kodric-Brown), pp. 120–131. John Wiley & Sons,  
655 Ltd, Chichester, UK.

656 Storch, D., Bohdalková, E. & Okie, J. (2018) The more-individuals hypothesis revisited: the role  
657 of community abundance in species richness regulation and the productivity–diversity  
658 relationship. *Ecology Letters*, **21**, 920–937.

659 Sullivan, B.L., Aycrigg, J.L., Barry, J.H., Bonney, R.E., Bruns, N., Cooper, C.B., Damoulas, T.,  
660 Dhondt, A.A., Dietterich, T., Farnsworth, A., Fink, D., Fitzpatrick, J.W., Fredericks, T.,  
661 Gerbracht, J., Gomes, C., Hochachka, W.M., Iliff, M.J., Lagoze, C., La Sorte, F.A.,  
662 Merrifield, M., Morris, W., Phillips, T.B., Reynolds, M., Rodewald, A.D., Rosenberg,  
663 K.V., Trautmann, N.M., Wiggins, A., Winkler, D.W., Wong, W.-K., Wood, C.L., Yu, J.  
664 & Kelling, S. (2014) The eBird enterprise: An integrated approach to development and  
665 application of citizen science. *Biological Conservation*, **169**, 31–40.

666 Thorup, K., Tøttrup, A.P., Willemoes, M., Klaassen, R.H.G., Strandberg, R., Vega, M.L., Dasari,  
667 H.P., Araújo, M.B., Wikelski, M. & Rahbek, C. (2017) Resource tracking within and  
668 across continents in long-distance bird migrants. *Science Advances*, **3**, e1601360.



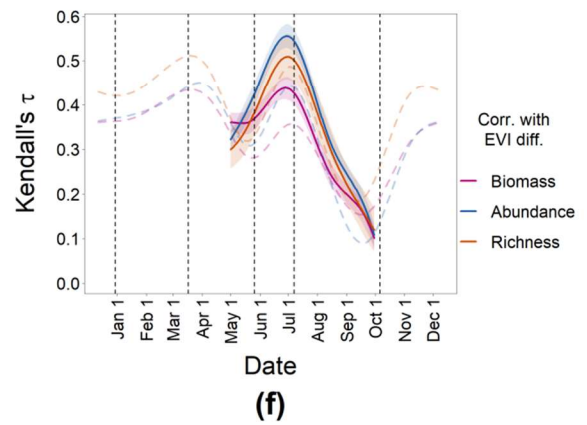
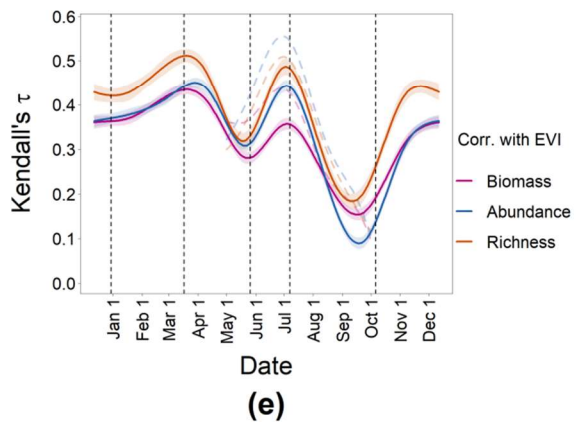
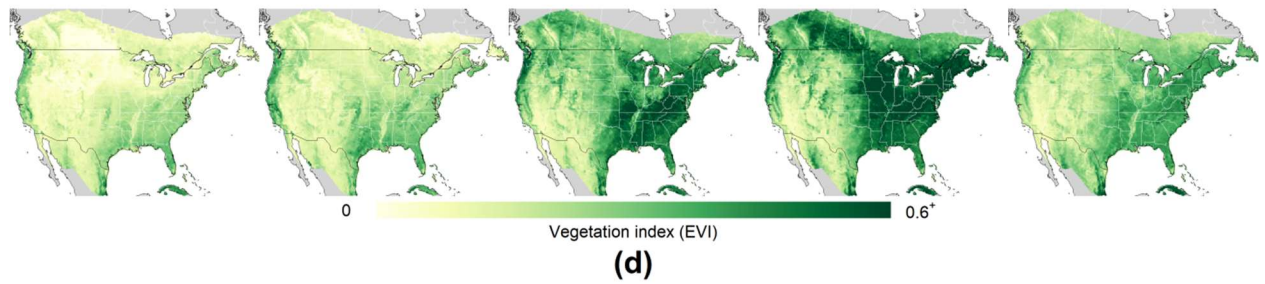
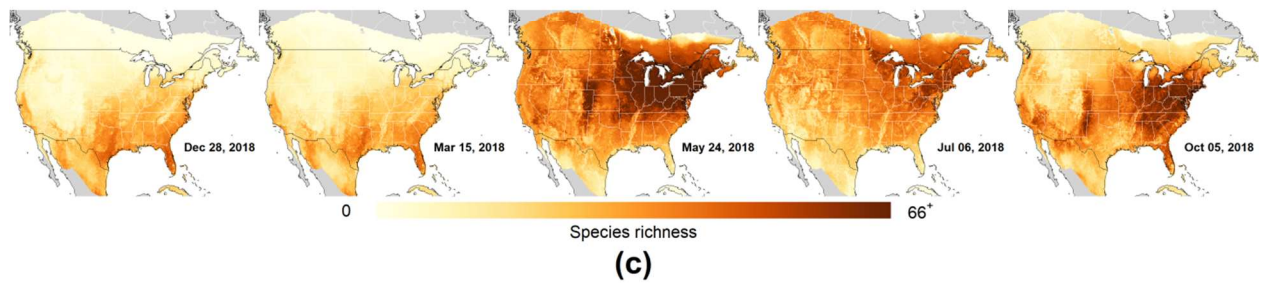
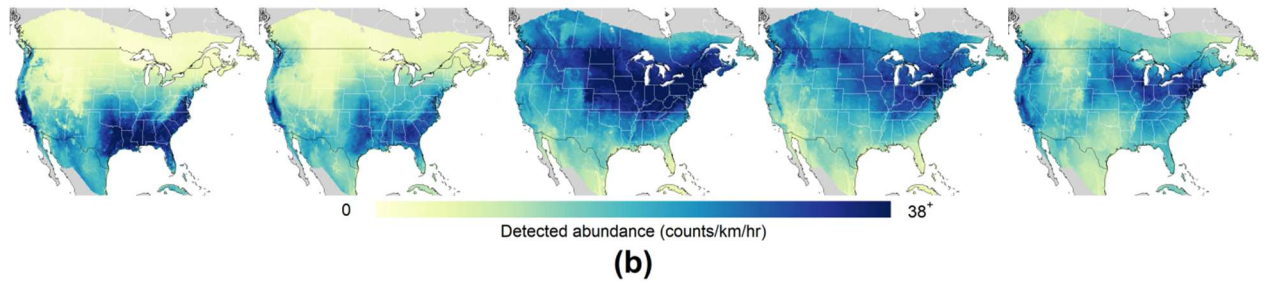
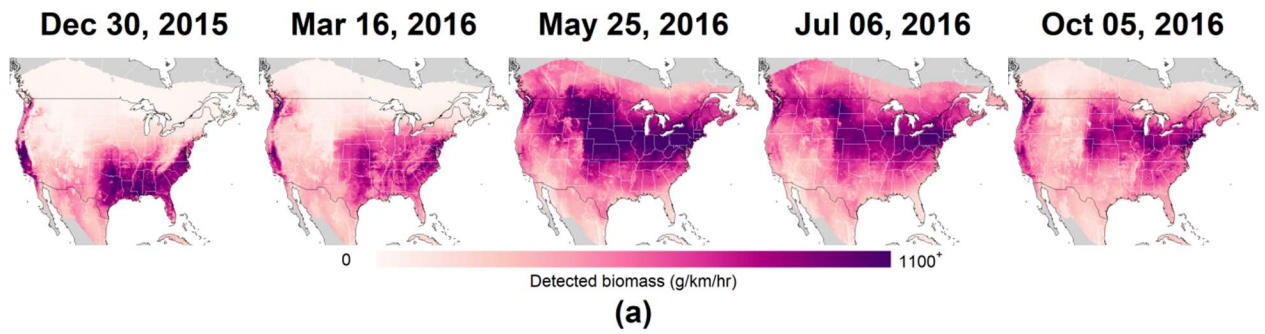
- 669 VanDerWal, J., Falconi, L., Januchowski, S., Shoo, L. & Storlie, C. (2014) *SDMTools: Species*  
670 *Distribution Modelling Tools: Tools for processing data associated with species*  
671 *distribution modelling exercises*. <http://www.rforge.net/SDMTools>  
672 Wood, S.N. (2017) *Generalized additive models: an introduction with R*, Second edition. CRC  
673 Press/Taylor & Francis Group, Boca Raton.  
674 Wright, D.H. (1983) Species-Energy Theory: An Extension of Species-Area Theory. *Oikos*, **41**,  
675 496.  
676 Wright, M.N. & Ziegler, A. (2017) ranger: A Fast Implementation of Random Forests for High  
677 Dimensional Data in C++ and R. *Journal of Statistical Software*, **77**, 1–17.

678

### 679 **Data accessibility statement**

680 The estimates of total biomass, abundance and species richness derived from eBird data, as well as EVI  
681 and bioclimatic variables extracted from publicly-available data sources, are available from Figshare at  
682 <https://doi.org/10.6084/m9.figshare.15085275.v1>.

683



685 **Figure 1 | Spatial associations between primary productivity and the biomass, abundance, and species**  
686 **richness of nocturnally migrating landbirds. (a)** Spatial distributions of total detected biomass estimated  
687 at five dates in 2016 representing different points of the annual cycle: winter (Dec 30), early spring  
688 migration (Mar 16), late spring migration (May 25), summer (July 06), and autumn migration (Oct 05). **(b)**  
689 Spatial distributions of total detected abundance at the same 2016 dates. **(c)** Species richness at the  
690 closest equivalent 2018 dates. **(d)** Primary productivity estimated using the MODIS Enhanced Vegetation  
691 Index (EVI) at the same 2016 dates. To avoid visual artifacts when comparing between maps, we used  
692 linear color scales (truncated at the 98 percentile) for all four quantities. **(e)** Spatial cross-correlation  
693 coefficients between EVI and biomass, abundance, and species richness across the study area, calculated  
694 weekly across the annual cycle. Vertical dashed lines correspond to the five dates. To reduce clutter, we  
695 only show the fitted lines and 95% confidence bands (as shaded regions) from generalized additive models  
696 (GAM); see Supp. Figure S5 for the actual correlation coefficients. **(f)** Similar to (e), except the spatial  
697 correlation is with the seasonal EVI difference, defined as EVI minus the site minima. To facilitate  
698 comparison between (e) and (f) while avoiding plot clutter, the lines in (e) have been reproduced as lighter  
699 dashed lines in (f), and vice versa. Additional maps and correlation coefficient curves can be found in Supp.  
700 Figure S3.

701

702

703

704

705

706

707

708

709

710

711

712

713

714

715

716

717

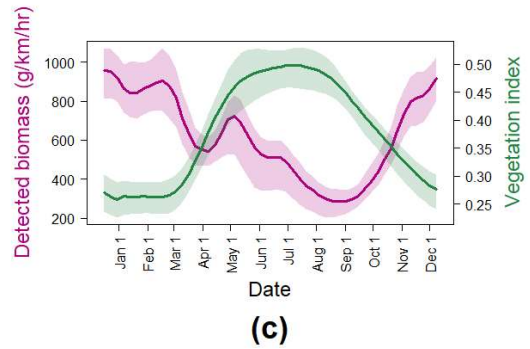
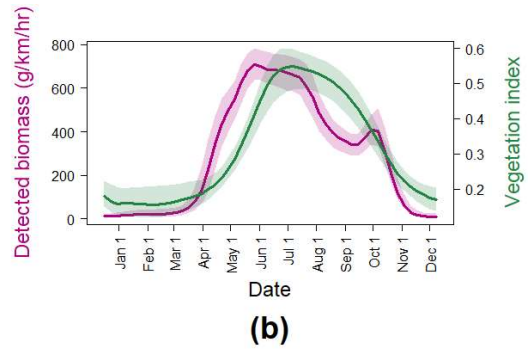
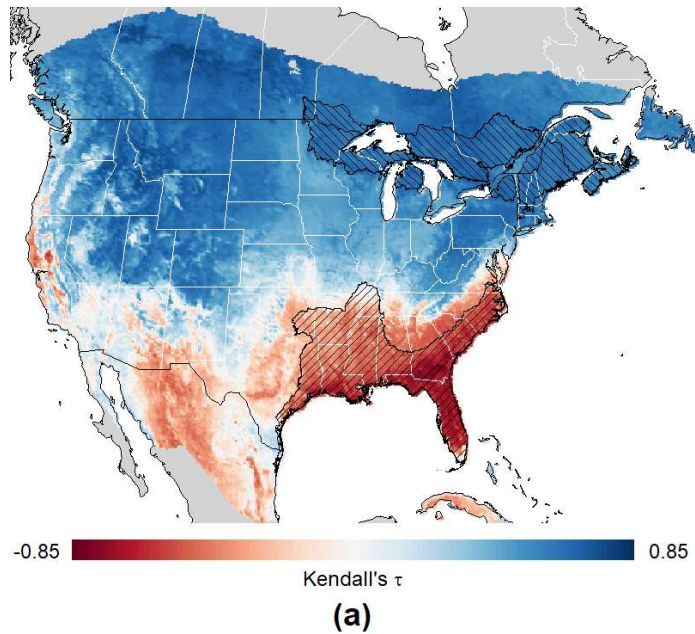
718

719

720

721

722



723

724 **Figure 2 | Temporal association between primary productivity and avian biomass.** (a) The Kendall  
 725 correlation coefficient between the MODIS Enhanced Vegetation Index (EVI) and biomass across weeks at  
 726 individual grid locations. Weekly median EVI and biomass across the (b) Northeast (blue hatched region)  
 727 and (c) Southeast (red hatched region). The regions were defined using combinations of Bird Conservation  
 728 Regions (see Methods for details). The colored bands in (b) and (c) indicate the interquartile ranges. See  
 729 Supp. Figure S7 for the abundance counterpart.

730

731

732

733

734

735

736

737

738

739

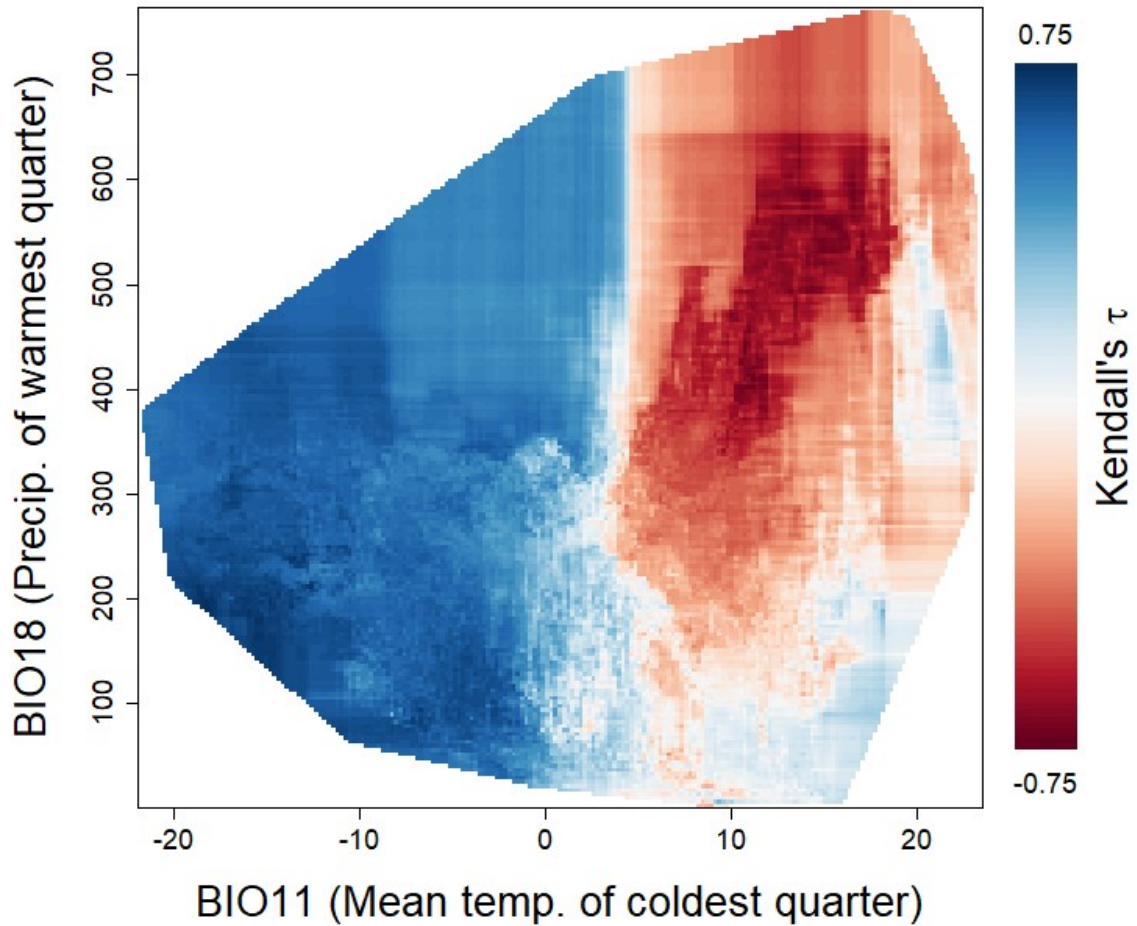
740

741

742

743

744



745

746 **Figure 3 | Explaining the spatial patterns of temporal associations using bioclimatic variables.** This figure  
 747 shows the dependence of the local EVI-biomass correlations on the two bioclimatic variables with the  
 748 highest importance (chosen using forward stepwise selection), estimated using a two-variable random  
 749 forest. The two variables are mean temperature of coldest quarter (BIO11) and precipitation of warmest  
 750 quarter (BIO18). We restricted the plot region to the convex hull of the data distribution to avoid over-  
 751 extrapolation.

752

753

754